

Probability of Dimer Formation on a Honeycomb Lattice

Zbigniew Domański, Zhibing Li and Yong Zhang

Abstract—Atoms adsorbed on a honeycomb lattice diffuse and eventually form dimers. Three types of dimers are possible with this lattice’s symmetry: ortho-, meta- and para-dimer. We estimate the probability of para- and ortho-dimer formation when atoms jump independently between sites of the underlying lattice. Our analyze is based on a simple model of diffusive motion of a pair of atoms which bind to lattice sites separated by a distance Δ , measured as a number of edges between sites and characterized by a chirality coefficient χ . Because of diffusive motion of atoms, Δ and χ change in time and we trace a flow over the configurational space. The flow eventually converges to one of possible absorbing states. If the particular adsorbing state is reached it means that a dimer corresponding to this state is formed. We have computed time-dependent probabilities P_O and P_P for ortho- and para-dimer formation, respectively. We have found that $4/15 < P_O/P_P < 5/14$.

Index Terms—chirality, diffusion, dimer, honeycomb lattice, random walk.

I. INTRODUCTION

ADSORPTION of atoms on plane lattices is a process of great importance in nanotechnology. A prominent example is adsorption of atomic hydrogen on graphene with prospective applications in low-scale-electronics [1], [2]. This phenomenon is also interesting in conjunction with hydrogen storage for subsequent use.

The adsorption of atoms on honeycomb lattices has gained attention because of their structural and chemical simplicity as models for the study of fundamental surface processes. Examples include formation and conversion of dimers or emergence of chiral properties due to the loss of mirror symmetry in the adsorbate – substrate system [4], [5], [6], [7].

For the purpose of this study a complex process of dimer formation will be reduced to a random walk process involving point-like atoms which jump between nodes of honeycomb lattice. Dimers are energetically more stable than the monomers and thus, within such a scenario, a dimer is formed when the relative positions of two atoms correspond to one of three arrangements presented in Fig. 1. Here, we take into account only the short dimmers. Extended dimers can also be considered, e.g. a number of extended hydrogen dimer configurations on graphite surface was reported in [3].

The mathematics behind our description relies on cellular automata network dynamics. We employ a language of a random walk in a space with absorbing states. An ensemble

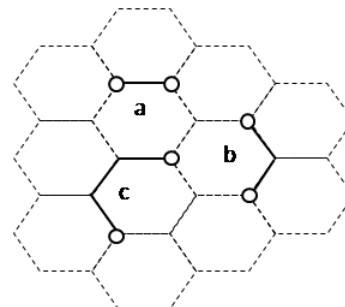


Fig. 1. Three different dimers on hexagonal lattice: (a) ortho-dimer, (b) meta-dimer, (c) para-dimer. Open circles mark the molecule positions and the solid lines are only visual guides

of all dimer configurations is represented by a set of disjoint classes of configurations characterized by chiralities of all possible node-to-node arrangements [7].

Consider a pair of atoms related to different nodes of honeycomb lattice. They are separated by a distance Δ being the number of edges along the shortest path between the nodes. At each time step the atoms jump independently and the distance Δ updates to new value:

$$\Delta \longrightarrow \Delta' \in \{\Delta - 2, \Delta, \Delta + 2\}. \quad (1)$$

The distance Δ , however does not supply all necessary information about the atom-to-atom arrangement. It is because the same value of Δ corresponds to $(\Delta + 1)/2$ (odd Δ) or $\Delta/2$ (even Δ) different arrangements. Examples of arrangements with odd values of Δ are presented in Fig. 2. Equation (1) shows that the simultaneous jump of atoms conserves parity of Δ . It means that such a diffusive motion keeps a pair of atoms within an ensemble of configurations with the parity fixed by initial atoms’ positions, i.e. the nodes to which they binded when the adsorption took place. Therefore each value of $\Delta = 2p + 1$ represents an ensemble of p configurations $\{\Delta_1 \equiv \Delta_z, \Delta_2, \dots, \Delta_p \equiv \Delta_a\}$ each of which is characterized by a chirality angle θ (see Fig. 3). We call such an ensemble the chirality class χ_Δ .

This chirality-class concept can be used to detect a dimer formation in a following way: if two atoms happen to reach one of χ_1, χ_2 chirality class or the configuration $\mathcal{3}_A$ from χ_3 they merge irreversibly forming a dimer.

In this paper we concentrate on ortho- and para-dimers and we relate probabilities of their formations with initial positions of atoms.

II. RANDOM WALK IN CHIRALITY SPACE

To see how diffusive motion of molecules is perceived from the chirality space perspective let us consider two atoms sitting at time τ at sites separated by Δ . To be specific, we

Manuscript received August 5, 2015.

Z. Domański is with the Institute of Mathematics of Czestochowa University of Technology, PL-42201 Czestochowa, Poland e-mail: zbigniew.domanski@im.pcz.pl.

Z. Li is with School of Physics and Engineering, Sun Yat-sen University, Guangzhou, 510275, P.R. China e-mail: stslzb@mail.sysu.edu.cn

Y. Zhang is with School of Physics and Engineering, Sun Yat-sen University, Guangzhou, 510275, P.R. China e-mail: zhyong9@mail.sysu.edu.cn

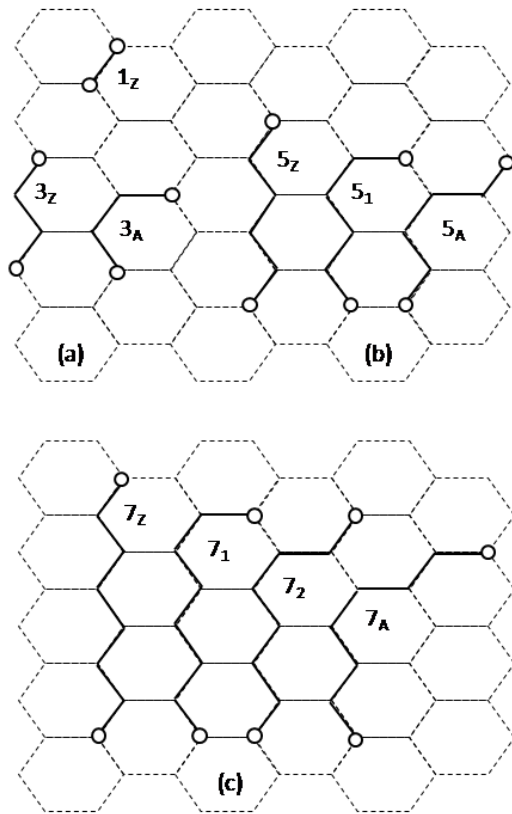


Fig. 2. Pairs of atoms on honeycomb lattice with separations 1, 3, 5 and 7: (a) two $\Delta = 3$ configuration, 3_Z (zig-zag) and para-dimer (P) (being 3_A armchair configuration); (b) three $\Delta = 5$ configurations, i.e. 5_Z (zig-zag), 5_1 and 5_A (armchair); (c) $\Delta = 7$ with its four configurations: 7_Z (zig-zag), 7_1 , 7_2 and 7_A (armchair). The only one $\Delta = 1$ configuration 1_Z , representing the ortho-dimer O , is shown in (a). Open circles mark positions of atoms and the solid lines are only visual guides

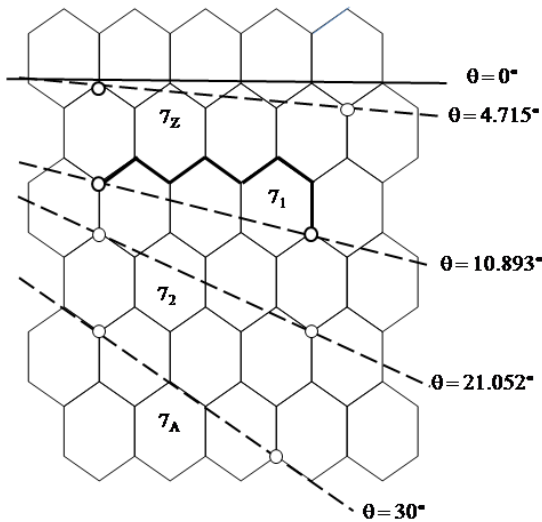


Fig. 3. Chirality class χ_7 with its four configurations: 7_Z (Zig-zag), 7_1 , 7_2 and 7_A (Armchair) and corresponding chiral angles θ . Open circles represent adsorbed atoms

take here $\Delta = 5$. At time $\tau + 1$ atoms jump independently to new nodes. There is no bias so each atom choses one of three its neighboring nodes with probability $1/3$. Since the atoms move independently then, after the jump they can be in one of 9 equally probable new node-to-node configurations

which belong to chirality classes χ_3, χ_5 and χ_7 . Closer look at these 9 configuration enable us to trace links along which configurations from the class χ_5 disperse among the classes χ_3, χ_5 and χ_7 . For this particular $\Delta = 5$ case links from $5_Z, 5_1$ and 5_A are presented in Fig. 4. Such a series of links can be constructed virtually for any Δ , although it can be a tedious job.

Diagrams in Figs. 4 and 5 contain information sufficient to built up a chain of recursive relations which starts at a configuration within a given chirality class and ends at P (para-dimer) or at O (ortho-dimer). Configurations P and O are the absorbing states in the chirality space. It is interesting to note that the absorbing state P can be reached from configuration 3_z with the probability $2/9$, once the configuration 3_z is populated or, with the probability $1/9$ from the configuration 5_A if there is a pair of atoms in this configuration (see Fig. 4c). It means that there are two independent pathways enabling para-dimer creation whereas only one pathway $3_z \rightarrow O$, with conditional probability $1/9$, points to the ortho-dimer formation (see Fig. 5). Each of these pathway is spanned by the links between consecutive classes $\chi_1, \chi_3, \dots, \chi_\mu$ (where μ is related to the lattice extension and to the life time of adsorbed atom [4]).

Before we employ the above mentioned pathways to estimate the probability of accessing the absorbing states P and O , we have to analyze how the configuration 5_A behaves on the pathway going to P . The diagram (c) in Fig. 4 shows that the vertex 5_A has no loop. It implies that the conditional probability $P(5_A|5_A)$ for 5_A stays active, if it was active in the precedent time step, equals to zero and thus, 5_A is a transitive state with no internal dynamics. Therefore, the pathway going to P via 5_A is open only if 5_A is constantly activated by 5_1 (with the probability $2/9$ as seen from the Fig. 4(b) and some configurations from the class χ_7 , namely 7_1 and 7_A (not shown here).

III. PROBABILITY FUNCTIONS FOR ORTHO- AND PARA-DIMER FORMATIONS

When two atoms are adsorbed on the lattice their relative initial positions correspond to a configuration Δ_l ($0 \leq l \leq (\Delta - 1)/2$) from the chirality class χ_Δ . Then, this initial configuration starts to flow in the chirality space and eventually reaches one of the absorbing states O or P . Therefore, our quantities of interest are the probabilities $P_O(\tau)$ and $P_P(\tau)$ for the two-atom-configuration Δ reaches chirality class χ_1 or the configuration 3_A (from the class χ_3), respectively. In other words $P_O(\tau)$ and $P_P(\tau)$ are the probabilities that two atoms merge irreversibly forming a dimer. Last two stages of such a flow are presented in Fig. 6. The flow diagram depicted in Fig. 6 can be considered as a rough approximation to the process. Within this approximation we keep an exact structure of relations inside of χ_1 and χ_3 classes whereas relations involving remaining chirality classes are reduced to links between χ_3 and an effective class denoted by the symbol Σ in Fig. 6. It means that detailed structure of relations among chirality classes $\chi_5, \chi_7, \dots, \chi_\mu$ is wrapped into the effective class Σ .

In this spirit, the probability $P_P(\tau)$ for such a flow of conversions of $\Delta_{l>3}$ when starting at $\tau = 0$ will be captured by P at time τ can be written in the following form

$$P_P(\tau) = P(P|3z) \cdot P_{3z}(\tau - 1) + P(P|\Sigma) \cdot P_\Sigma(\tau - 1), \quad (2)$$

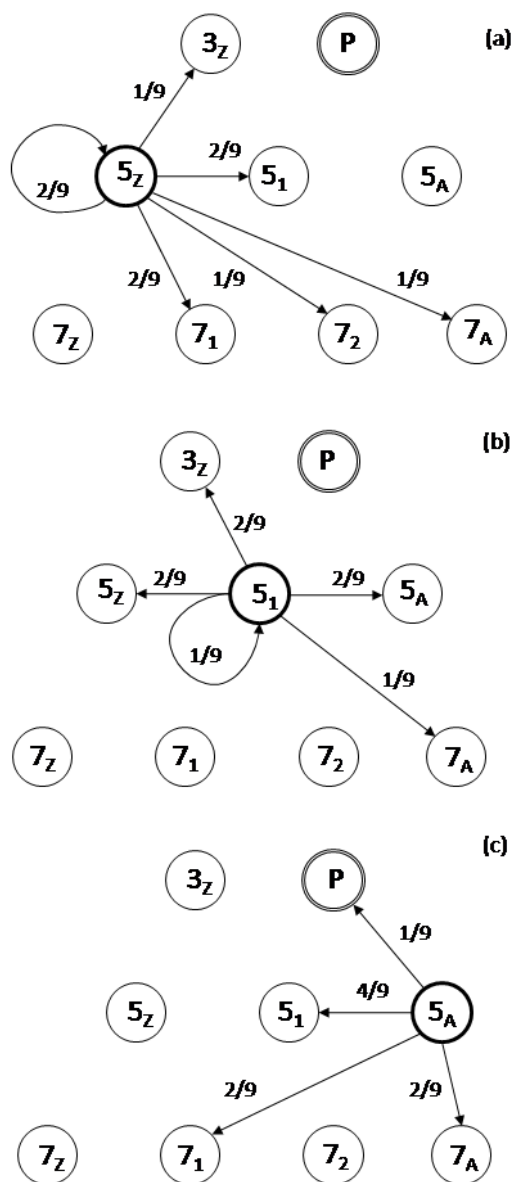


Fig. 4. Schemes of dispersion of chirality class χ_5 : (a) configuration 5_Z , (b) configuration 5_1 and (c) configuration 5_A . Arrows and labels indicate target configurations and conditional probabilities of corresponding conversions, respectively. Double circle is the absorbing configuration P representing the para-dimer

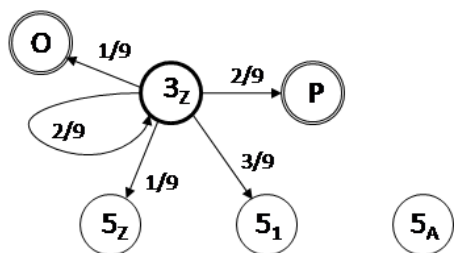


Fig. 5. Same description as in the Fig. 4: configuration 3_Z from the chirality class χ_3 . Double circles: O and P state for ortho- an para-dimer absorbing configurations, respectively

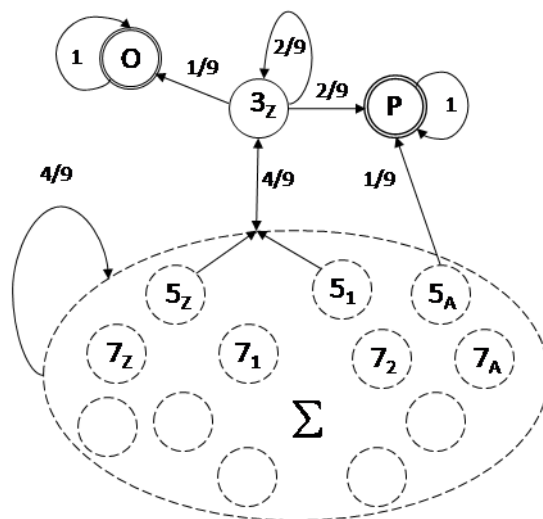


Fig. 6. Flow diagram in the chirality space. Two last stages before a dimer formation are shown. Double circles indicate absorbing configurations O and P . Links between chirality classes follow links shown in Figs. 4-5. Symbol Σ denotes the set of all chirality classes except classes χ_1 and χ_3

where $P(\alpha|\beta)$ denotes the conditional probability that the atoms jump from a configuration β to α . $P(\alpha|\beta)$ can also be seen as a rate of conversion of the configuration β into the configuration α once β is populated. Since there is only one pathway to ortho-dimer formation then the probability P_O is given by

$$P_O(\tau) = P(O|3_Z) \cdot P_{3_Z}(\tau - 1). \quad (3)$$

We see that $P_P(\tau)$ as well as $P_O(\tau)$ depend on the same pair of probability functions: P_{3_Z} and P_Σ evaluated at the preceding time $\tau - 1$. It means that our approximation reduces original random walk in chirality classes to the random walk between two point-like classes Σ and 3_Z plus two absorbing configurations O and P . The probabilities $P_{3_Z}(\tau)$ and $P_\Sigma(\tau)$ depend on their values in previous time in a following way

$$P_{3_Z}(\tau) = P(3_Z|3_Z) \cdot P_{3_Z}(\tau - 1) + P(3_Z|\Sigma) \cdot P_\Sigma(\tau - 1), \quad (4)$$

$$P_\Sigma(\tau) = P(\Sigma|3_Z) \cdot P_{3_Z}(\tau - 1) + P(\Sigma|\Sigma) \cdot P_\Sigma(\tau - 1). \quad (5)$$

Since these functions characterize non-absorbing states of our chirality network then they are a self-sustained pair of time dependent quantities. Therefore, their particular forms can be evaluated in a chain-like manner starting from the initial values $P_{3_Z}(\tau = 0)$ and $P_\Sigma(\tau = 0)$.

To see that let us rewrite the Eqs. (2)-(5) as a matrix-vector equation

$$\mathcal{P}(\tau) = \mathbf{T} \cdot \mathcal{P}(\tau - 1) = \dots = \mathbf{T}^\tau \cdot \mathcal{P}(0) \quad (6)$$

where the vectors of probability functions $\mathcal{P}(\tau)$ and $\mathcal{P}(0)$ are

$$\mathcal{P}(\tau) = \begin{pmatrix} P_O(\tau) \\ P_P(\tau) \\ P_{3_Z}(\tau) \\ P_\Sigma(\tau) \end{pmatrix}, \quad \mathcal{P}(0) = \begin{pmatrix} 0 \\ 0 \\ 0 \\ 1 \end{pmatrix}. \quad (7)$$

Entries of the transfer matrix \mathbf{T} are the appropriate conditional probabilities marked in the Fig. 6, i.e.

$$\mathbf{T} = \begin{bmatrix} 1 & 0 & 1/9 & 0 \\ 0 & 1 & 2/9 & 1/9 \\ 0 & 0 & 2/9 & 4/9 \\ 0 & 0 & 4/9 & 4/9 \end{bmatrix}. \quad (8)$$

The particular form of $\mathcal{P}(0)$ reflects our assumption that the initial positions of atoms are separated by $\Delta > 3$ and thus $P_O(0) = P_P(0) = P_{3z}(0) = 0$. The nonsingular matrix \mathbf{T} can be easily diagonalized. Its spectrum is the set of numbers $\{1, 1, \lambda_-, \lambda_+\}$ where

$$\lambda_{\mp} = \frac{1}{3} \mp \frac{\sqrt{17}}{9} \quad (9)$$

and thus the τ -th power of \mathbf{T} is given by

$$\mathbf{T}^\tau = \mathbf{S}^{-1} \cdot \begin{bmatrix} 1 & 0 & 0 & 0 \\ 0 & 1 & 0 & 0 \\ 0 & 0 & \lambda_-^\tau & 0 \\ 0 & 0 & 0 & \lambda_+^\tau \end{bmatrix} \cdot \mathbf{S}, \quad (10)$$

with

$$\mathbf{S} = \begin{bmatrix} 1 & 0 & 5/9 & 4/9 \\ 0 & 1 & 14/9 & 15/9 \\ 0 & 0 & -1 + \lambda_-/4 & 0 \\ 0 & 0 & 0 & -1/2 + \lambda_+/4 \end{bmatrix}, \quad (11)$$

Explicit forms of \mathbf{T}^τ , Eq. (10) and $\mathcal{P}(\tau)$, Eq. (7), yield the time dependent probabilities $P_O(\tau)$ and $P_P(\tau)$ in terms of $\mathcal{P}(0) = (0, 0, 0, 1)$, namely

$$P_O(\tau) = \frac{4}{19} + \frac{5\sqrt{17} - 11}{19(17 + \sqrt{17})} \lambda_-^\tau - \frac{23 + 7\sqrt{17}}{19(17 + \sqrt{17})} \lambda_+^\tau \quad (12)$$

$$P_P(\tau) = \frac{15}{19} + \frac{4(7\sqrt{17} - 23)}{19(17 + \sqrt{17})} \lambda_-^\tau - \frac{163 + 43\sqrt{17}}{19(17 + \sqrt{17})} \lambda_+^\tau \quad (13)$$

as well as the functions $P_{3z}(\tau)$ and $P_\Sigma(\tau)$

$$P_{3z}(\tau) = \frac{2}{\sqrt{17}} (\lambda_+^\tau - \lambda_-^\tau) \quad (14)$$

$$P_\Sigma(\tau) = \frac{8}{17 + \sqrt{17}} \lambda_-^\tau + \frac{9 + \sqrt{17}}{17 + \sqrt{17}} \lambda_+^\tau \quad (15)$$

As an example the function $P_O(\tau)$ is shown in Fig. 7.

Although $\mathcal{P}(\tau)$ can be written for a general initial distribution $\mathcal{P}(0)$, i.e. $\mathcal{P}(0) = (0, 0, P_{3z}(0), P_\Sigma(0))$, the overall characteristic of dimer formation can be seen already from Eqs. (12) - (15) which are valid only for $\mathcal{P}(0) = (0, 0, 0, 1)$. Since $|\lambda_{\mp}| < 1$ then, for $\tau \gg 1$, we have the following relation among the probabilities of dimer formation

$$\frac{P_O(\tau)}{P_P(\tau)} \approx \frac{4}{15} + \frac{1}{15} \left(1 + \frac{52}{15\sqrt{17}} \right) \lambda_+^\tau \longrightarrow \frac{4}{15}. \quad (16)$$

If the initial configuration is a mixture of Δ_{3z} and Δ_Σ configurations with probabilities p and $1 - p$, respectively then $\mathcal{P}(0) = (0, 0, p, 1 - p)$ and the ratio of probabilities stays within the range

$$\frac{4}{15} < \frac{P_O(\tau)}{P_P(\tau)} < \frac{5}{14} \quad (17)$$

when $\tau \rightarrow \infty$.

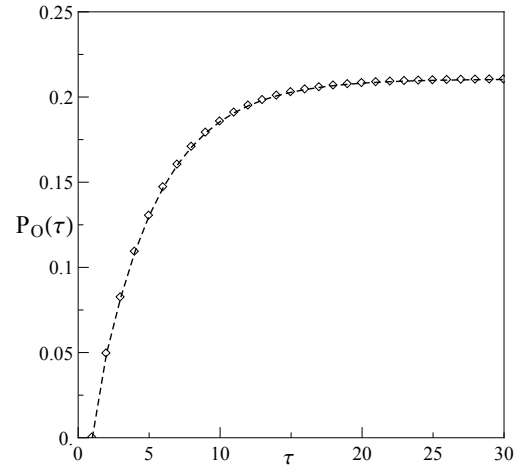


Fig. 7. Discrete-time probability function $P_O(\tau)$ of the ortho-dimer formation given by Eq. (12). Dashed line is a visual guide

IV. CONCLUSION

Our analytical approach relies on assumption that the dimers appear due to sequences of synchronous jumps of atoms. We are perfectly aware that such an assumption does not reflect displacement of adsorbed atoms in a real system. It is mainly because atoms do not move simultaneously. They change positions at different times. Our toy model, however yields some valuable information because the coherent movement of atoms can appear in the proximity of one of the adsorbing states. A few steps before the dimer formation, when the atoms are relatively close to each other, they correlate their jumps and the rate at which a particular dimer appears can be described within the scenario resulting from our model. Obviously, more detailed description of the random walk is necessary, i.e. more than two chirality classes should be considered in conjunction with distributions of distances in hexagonal lattices [7], [8]. Apart from the hopping time also a residence time have to be included into the model because the time of residence is substantially longer than the time of hopping from one lattice node to another.

REFERENCES

- [1] D.C. Elias, R.R. Nair, T.M.G. Mohiuddin, S.V. Morozov, P. Blake, M.P. Halsall, A.C. Ferrari, D.W. Boukhvalov, M.I. Katsnelson, A.K. Geim and K.S. Novoselov, "Control of Graphene's Properties by Reversible Hydrogenation: Evidence for Graphane," *Science*, vol. 323, p. 610-613 (2009).
- [2] A. Savchenko, "Transforming Graphene," *Science*, vol. 323, pp. 589-590 (2009).
- [3] Z. Sljivancanin, E. Rauls, L. Hornekaer, W. Xu, F. Besenbacher and B. Hammer, "Extended atomic hydrogen dimer configurations on the graphite (0001) surface," *J. Chem. Phys.* vol. 131, 084706 (2009).
- [4] Y. Xia, W. Wnag, Z. Li and H. J. Kreuzer, "Adsorption and desorption of hydrogen on graphene with dimer conversion," *Surface Science*, vol. 617, pp. 131-135 (2013).
- [5] J.O. Sofo, A.S. Chaudhari and G.D. Barber, "Graphane: A two-dimensional hydrocarbon," *Phys. Rev. B*, vol. 75, 153401 (2007).
- [6] H. Arce, W.L. Mochán and J.J. Gutiérrez, "Minimum energy 2D patterns of atoms adsorbed on a hexagonal lattice," *Surface Science*, vol. 348, pp. 379-386 (1996).
- [7] N.V. Richardson, "Adsorption-induced chirality in highly symmetric hydrocarbon molecules: lattice matching to substrates of lower symmetry," *New J. Phys.*, vol.9, 395 (2007).
- [8] Z. Domański and N. Szczygiol, "Distribution of the Distance Between Receptors of Ordered Micropatterned Substrates," In: *Transactions on Engineering Technologies*, Volume 170, H.K. Kim, S.-I. Ao and B. Rieger (eds.), Springer, pp. 297-308 (2013).